

Electrografting of 3-aminopropyltriethoxysilane on HOPG.

Diana Méndez Arvelo

Facultad de Ciencias-
Universidad de La Laguna.

Master in Molecular
Nanoscience and
Nanotechnology

Course: 2020-2021

Supervisors: Alejandro González Orive, Alberto Hernández Creus.

Modification of graphene-like surfaces is useful to change their inherent surface chemistry such as inertness and poor adhesion, but without altering properties of interest. In this work, given the bifunctional nature of the APTES (3-Aminopropyltriethoxysilane) molecule, we propose two electrografting methods to covalently attach either silane groups or amine groups to a HOPG electrode, based on sol-gel and electrochemical self-assembly methodologies, respectively. The formation and growth of the as-prepared films is monitored by using atomic force microscopy (AFM) and cyclic-voltammetry (CV) in the presence of an electrochemical redox probe. AFM imaging showed the formation of ultrathin films with differential morphologies and thicknesses depending on the grafting method. The surface chemical composition of the films has been characterized by attenuated total reflectance-Fourier transform infrared (ATR-FTIR) and Raman Spectroscopy.

Introduction

Organosilanes are hybrid molecules that contain in their structure at least one hydrolysable alkoxy silane, being their general formula $R-Si(OR)_3$. It is usual that they bear organic functionalities, i.e. vinyl, epoxy, amines or mercapto¹. As such, they can be deposited on different substrates: glass, metallic or even polymeric surfaces. In this way, these molecules have been traditionally used for different applications, which include preparation of composites, paints, adhesives, etc². Moreover, they can also alter the physicochemical and mechanical properties of the materials they are used with, including hydrophobicity, temperature, or abrasion resistance. One of the most important applications is as primers and adhesion promoters, allowing to improve interfacial adhesion, taking advantage of the different types of reactions that can be performed on organosilanes: hydrolysis, condensation (between themselves or with a substrate) and alcoholysis³.

More specifically, aminosilanes are widely used as coupling agents⁴, due to their bifunctional nature. Their

application in aqueous media has gained importance recently because of the increasing relevance of surface chemistry in life and environmental sciences⁵. The presence of the amine group provides these molecules with high reactivity. The lone pair of electrons of the nitrogen atom of the amine group permits a hydrogen bonding interaction with hydrogen donating groups, as other amines or hydroxyl groups, which makes aminosilanes water-soluble and allows fast absorption of the amine groups to substrate surface rich with hydroxyl groups⁶. Aminosilanes are interesting for surface reaction chemistry since amine-catalyzed reactions of alkoxy groups with surfaces may lead to the formation of uniform films⁷. Applications of these molecules include: the use as foundation layer in biosensors⁸, the increase of adhesion in fiberglass-epoxy composites on silica surfaces⁹, suppress polymer film dewetting¹⁰, production of arrays of metal nanoparticles on silica substrates¹¹, and helping probe protein and cell adhesion¹².

3-Aminopropyltriethoxysilane (APTES) is one of the most used aminosilanes. As can be seen in Fig 1, this molecule contains three ethoxy groups per molecule

and is capable of polymerizing in the presence of water, which can give rise to several possible surface structures: chemisorbed layers by covalent attachment, two-dimensional self-assembly (horizontal polymerization), and multilayers (vertical polymerization). For this molecule to form multilayers in organic solvents the presence of a certain amount of water is required¹³. In this way, the number of protonated amines and hydrolyzed ethoxy groups will depend on the quantity of surface water¹⁴.

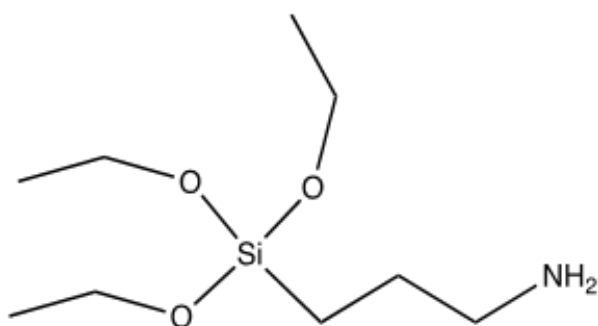


Fig 1. Molecular structure of the APTES molecule.

The use of APTES as a coupling agent is important for surface modification, mainly due to its terminal amine functionalities, that can be exposed to a gas or liquid phase for further modifications, allowing the attachment of molecules and self-assembly¹⁵. This process is also useful to improve the stability of a polymer/substrate interface in aqueous solutions because they are able to form covalent bonds with a hydroxylated surface¹⁶.

In some cases, the surface properties of different materials of interest are not convenient in terms of wettability, adhesion properties or biocompatibility. For that reason, they are needed to be modified for certain applications or further processing such as coating with functional materials¹⁷. In this way, surface modification methods are ideal for tuning surface properties of electrode materials, which enables a more precise control of the interfacial properties.

Particularly, electrografting is a method that provides robust, well-defined compositions and structures of

electrode interfaces, allowing to obtain the covalent attachment of organic compounds¹⁸.

Electrografting refers to the electrochemical reaction that permits the covalent binding chemisorption¹⁹ of organic layers to a solid substrate. This definition can be extended to reactions which involve an electron transfer between the substrate to modify the reagents. At the same time, it includes when a reducing or oxidizing reagent is added in order to produce the reactive species¹⁹. It can be applied to a wide variety of substrates including carbon²⁰, metals²¹, and their oxides²², as well as dielectrics such as polymers. This process implies an electrochemical reaction and indeed, an electron transfer, so the substrate will be connected to a potential generator¹⁹. Well-known electrografting methods include amines²³, carboxylates²⁴, Grignard reagents²⁵, diazonium salts²⁶, etc. Electrografting and related methods have been used for purely academic studies as well as for industrial applications, that include, among others: further modification of the electrografted layers, chemical sensors^{27,28}, biosensors²⁹, catalysis^{30,31}, etc.

Grafting of molecular layers to surfaces allows to control the interfacial properties and reactivities of the surfaces maintaining the properties of bulk materials. Graphitic carbons show many attractive characteristics, such as high mechanical stability and good electrical conductivity. These materials can be easily modified by methods that give very stable molecular coats, attached by strong C-C³² or C-N covalent bonds. In certain cases, these coatings have been proved to be largely unaffected by elevated temperatures³³. For electrochemical studies, the grafted layers have resisted wide potential ranges³⁴.

The substrate used in this work is a single crystalline Highly Oriented Pyrolytic Graphite (HOPG). This graphitic material includes basal plane and edge plane carbon sites in a spatial arrangement, and their relative abundance will depend on the quality of the specific crystalline substrate. The surface used exhibits mostly a

lower reactivity, hampering thus the covalent anchoring of molecules³⁵. Electrografting can then be used for the latter purpose in order to tune the interfacial properties, leading to different electrochemical applications, such as sensors and biosensors³⁶ or chemisorption of electroactive molecules of interest.

The -silane used in this work, APTES, shows two different functionalities: three ethoxy groups, that can be easily hydrolyzed to obtain silanol groups (Si-OH) to interact with the sample; and an amine group, whose electrografting mechanism on carbonaceous materials is well known. It is possible to bind either the silanol³⁷ or the amine³⁸ groups to the surface by controlling experimental conditions such as the applied voltage and pH, making APTES a good candidate as a multifunctional material.

Interestingly, although some reports have dealt over the last few years with the electrografting of APTES onto different surfaces, no significant effort has been made in order to characterize the nucleation and growth process and topographic features of the as-obtained films. With that aim, we have carried out in this work two different approaches for the electrografting of APTES onto a rather inert surface such as the basal plane of the HOPG. These atomically flat terraces would provide atomically flat terraces formed by C sp² hexagonal lattice terminated by C sp³ steps exhibiting different functionalities.

For that purpose, grafting through the amines as well as through silanol groups are performed on a HOPG electrode with different experimental conditions. The aim is in both cases the covalent bonding of the organic layer to the surface. The formation of these bonds is demonstrated by ATR-FTIR and Raman Spectroscopy. Moreover, the APTES-modified HOPG substrates were also characterized by cyclic-voltammetry (CV) and Atomic Force Microscopy (AFM). Either different deposition times or number of cycles were performed in order to provide a fundamental description of the growth and nucleation of the layers.

Experimental

Materials

3-Aminopropyltriethoxysilane (APTES, Sigma, 98%), tetrabutylammonium tetrafluoroborate (Bu₄N⁺BF₄⁻, Aldrich, 99%), acetonitrile (Riedel de Haën, 99,9%), ethanol (Scharlau, 96%), HNO₃ (Sigma-Aldrich, 65%), KCl (Acofarma, 99%), K₃[Fe(CN)₆] (Sigma-Aldrich, 99%), K₄[Fe(CN)₆] (Sigma-Aldrich, 98,5%), HOPG electrode, ultrapure water.

Electrochemical Methods

- Electrografting of APTES on HOPG.

The 3-aminopropyltriethoxysilane (APTES, used as received, 99%, Sigma-Aldrich) was electrografted on HOPG substrates by means of a three electrode-cell, with a calomel reference electrode (Radiometer Analytical, Hach Co. Loveland, CO, USA) and a platinum foil as counter-electrode. The freshly exfoliated HOPG substrates (See Fig S1 in SI) were employed as working electrodes. Two different approaches have been considered herein for the electrografting of APTES on HOPG.

The first method would imply a sol-gel methodology using an electrolyte solution made of 2.5% v/v APTES in 50:50 EtOH/H₂O, the pH was lowered by adding a 0.2 M KNO₃ solution until pH between 3-3.5. The resulting solution was hidden from light and stirred for 24 hours. The electrografting reaction was carried out using chronoamperometry (100 mV·s⁻¹), applying a constant potential, i.e. -1.2V for different deposition times (5 s, 10 s, 30 s and 60 s) showing the case for 30 s in Fig 2. The modified electrodes were rinsed abundantly with water and then treated at 80°C for 1 hour.

The electrolyte medium employed to perform the second electrografting was a 1 mM APTES solution in acetonitrile (ACN), containing 0.1 M tetrabutylammonium tetrafluoroborate (Bu₄N⁺BF₄⁻) as supporting electrolyte (TTBATFB4, >99%, Sigma-Aldrich). This solution was bubbled with Ar to remove the dissolved oxygen. The electrografting of the substrates was performed by cyclic voltammetry, applying a potential scan between +0.7 and +1.8 V (vs. SCE) at 100 mV·s⁻¹ for a growing number of cycles (1, 5,

and 10) shown in Fig 3. The modified electrodes were rinsed with acetone, ethanol and water and then treated at 85°C for 15 minutes.

After the grafting processes, the APTES-modified substrates were thoroughly rinsed with ACN and subsequently ultrasonicated in ACN for 5 min and dried under Ar stream. The as-prepared films were employed for the characterizations described in further sections.

Chronoamperometry (CA) and cyclic voltammetry (CV) experiments were performed with an Autolab potentiostat from Eco Chemie and a standard three-electrode cell.

- **Electrochemical characterization of APTES thin films on HOPG.**

For the electrochemical characterization of the as-prepared APTES thin films on HOPG, CV experiments have been carried out in a 1 mM ferrocyanide/ferricyanide-containing 0.1 M KCl aqueous solution.

Surface Analysis

- **Atomic Force Microscopy (AFM)**

AFM images were obtained in Tapping and Peak-Force modes using a Dimension ICON microscope equipped with a Nanoscope V control unit from Bruker operating in ambient air at a scan rate of 0.5–1.2 Hz, using RFESPA-75 (75–100 kHz, and 1.5–6 N·m⁻¹, nominal radius of 8 nm) and ScanAsyst-Air-HR (130–160 kHz, and 0.4–0.6 N·m⁻¹, nominal radius of 2 nm) cantilever/ tip assemblies, purchased from Bruker. Root Mean Squared (Sq) roughness, Bearing and Depth statistical analysis were carried out off-line with Nanoscope v. 2.0 and Gwyddion v. 2.59 software packages. The particle estimation was performed using the Grain Analysis tool after masking each particle individually using the Edit Mask Tool.

- **ATR-IR**

ATR-IR spectra of the APTES coatings were obtained with a IFS 66/ S Bruker Optics equipment with 512 scans per spectrum with a scan range of 4,000–600 cm⁻¹ and a resolution of 4 cm⁻¹. To this end, HOPG substrates were coated with APTES, while a second uncoated crystal was used as the reference. The spectra were obtained at the

same controlled environmental conditions, in order to subtract the effects of the environmental contributions and the pristine HOPG from the APTES coating spectra. The data were processed by Opus 6.5 software.

- **Raman Spectroscopy**

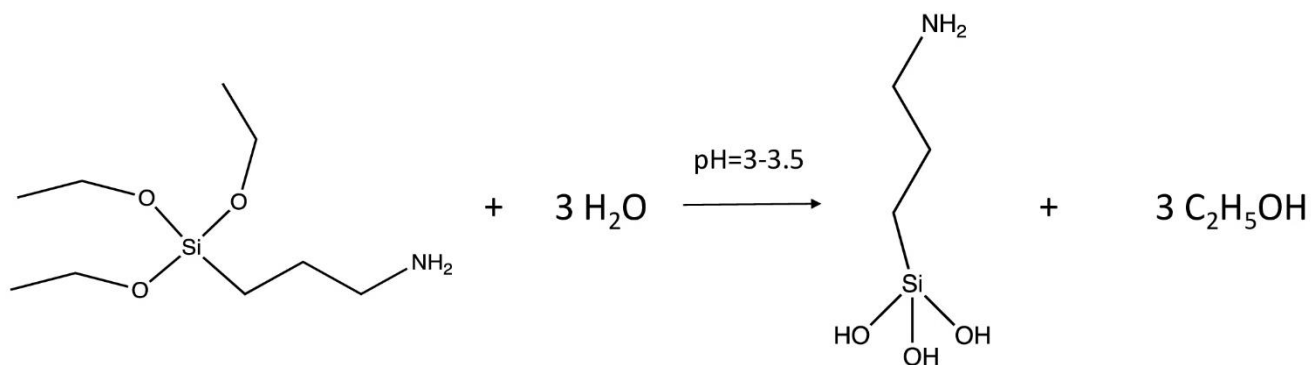
Raman spectra, used for the additional chemical characterization of the APTES-modified HOPG surfaces, were recorded with an InVia Renishaw Raman microscope (Renishaw, Germany) using a CCD detector, a YAG laser (532 nm, 55 mW max. power), and the corresponding gratings and filter. A 50x objective and 20 scans were employed for all measurements. The equipment was calibrated to the peak position of 520.0 cm⁻¹ (± 0.5 cm⁻¹) with a silicon wafer.

Results and Discussion

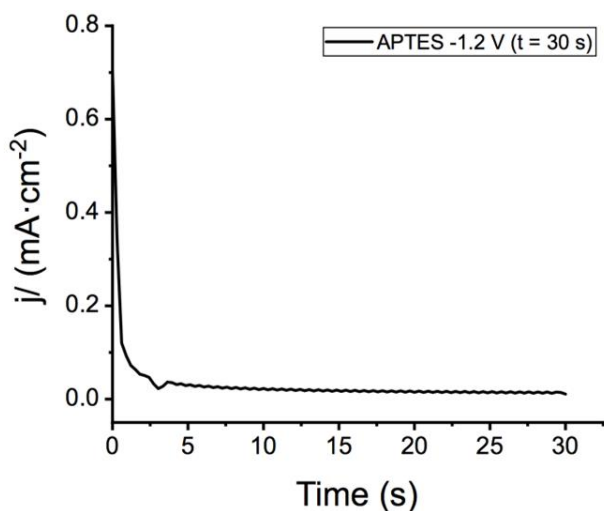
Film deposition through silane groups

To graft alkoxy silanes on a surface, a prehydrolysis step is needed to obtain the silanol groups (Si-OH) responsible for the covalent interaction with the substrate surface³⁹. Since the rate of the hydrolysis is much higher for acidic conditions than for basic, and the condensation of the hydroxyl groups is more likely to happen in basic mediums, this reaction will be performed using acidic conditions⁴⁰ since the rate of the hydrolysis is much higher. This step is summarized in Scheme 1.

A representative chronoamperometric curve registered for a deposition time at an applied potential of -1.2 V (vs. SCE) is displayed in Fig. 2. It shows the typical expected profile, i.e. a steep increase in the current density value is observed in the initial milliseconds corresponding to a capacitive behavior associated with the reorganization of the electrochemical double layer, followed by a rapid decrease until a diffusion-limited Faradaic current density value is achieved according to the Cottrell equation⁴¹.



Scheme 1. Pre-hydrolysis step catalysed in acidic medium.

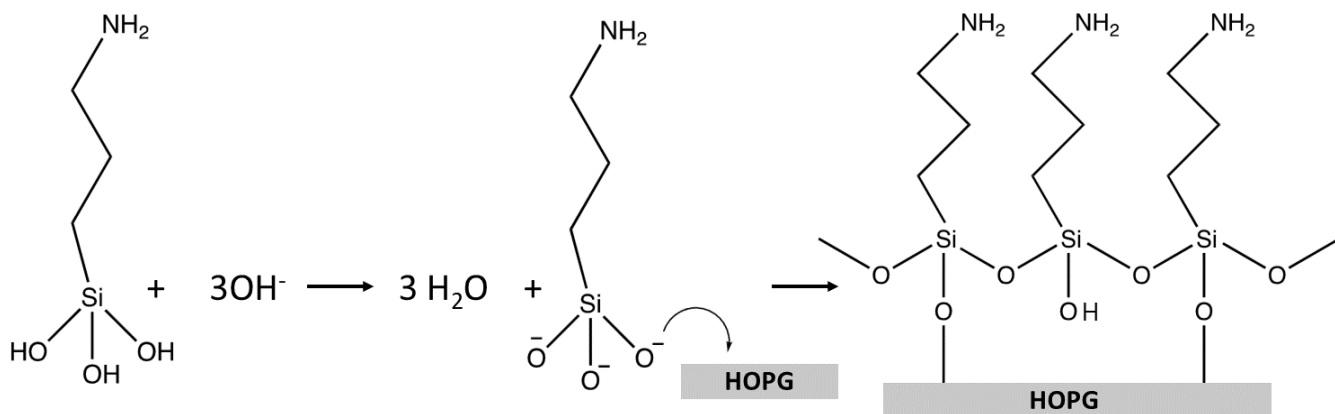
Fig 2. Chronoamperometric curve registered at -1.2 V (vs. SCE) for 30 s of deposition time in the APTES containing aqueous solution at a scan rate of 100 mV·s⁻¹.

In this step, the pH at the solid-liquid interface is locally increased by means of the electrochemical reduction of nitrate to nitrite ions present in the working electrolyte as shown in eq 1. The generated hydroxyl groups act as catalysts responsible for the polycondensation of the prehydrolyzed silanols to hydroxyl groups present on

the HOPG substrate and in between them. The voltage used is -1.2 V (vs. SCE), that has been checked by cyclic voltammetry to be within the potential range where this reduction happens (see Fig S2 in SI). More negative potentials could lead to Hydrogen Evolution Reaction (HER), that would locally increase the pH at the solid-liquid interface too, which is the desired effect. Nevertheless, the generation of H₂ bubbles would lead to the appearance of defects and pinholes in the formed films, affecting the homogeneity of the formed layers.



Polycondensation occurs only at the electrode surface where the necessary catalyst is electrogenerated and the layer deposition can be controlled by the deposition time as shown in Scheme 2. This polycondensation leads to the formation of a siloxane network (Si-O-Si) with loss of a water molecule of the corresponding alcohol. The final step is the formation of covalent bonds between the surface and the siloxane network, which finally leads



Scheme 2. Polycondensation of the silanol groups.

to the formation of a siloxane network strongly bonded to the surface⁴⁰. The process of nucleation during electrochemical deposition of the silanol groups occurs at active surface sites, which are supposed to be the steps in between terraces and defects in the structure. The fact that the voltage is applied to reduce the nitrates groups and not the organosilane itself, makes this process an indirect electrografting.

Film deposition through amine groups

The electrografting reaction through the amine groups was carried out by cyclic voltammetry scanning potentials between +0.7 and +1.8 V (vs. SCE), which has been proved to be the suitable window potential range for the electrooxidation of the primary amine³¹. An irreversible oxidation wave is observed in the first cycle at +1.2V (vs. SCE), Fig 3, which is attributed to the electrochemical oxidation of the amine groups to generate N-based radical species in the vicinity of the substrate surface according to Scheme 3. The significant decrease in the Faradaic current density observed in the following cycles would be indicative of the formation of non-conductive APTES-based thin films. Thus, as can be seen in Fig 7, the diffusion-controlled reversible electrochemical response exhibited by the pristine surface of the HOPG (black voltammogram) is progressively blocked by the presence of the APTES film.

The mechanism for the electrografting of primary amines was first described on glassy carbon and has been extended to other different surfaces¹². The electrooxidation of primary amines at carbon electrodes is chemically irreversible and leads to covalent grafting of an organic layer at the surface. It has been demonstrated^{42,43} that this electrooxidation yields the radical cation that quickly deprotonates giving a radical with tautomeric forms, as shown in Scheme 3. Once the electrografted molecules have started occupying the active surface sites, the oxidized amines would be more likely to attach to the ethoxy groups, leading to the formation surface attached layers⁴⁴. This mechanism states a clear difference with the silane grafting, since in this case the voltage is applied to oxidize the amine, being thus a direct electrografting.

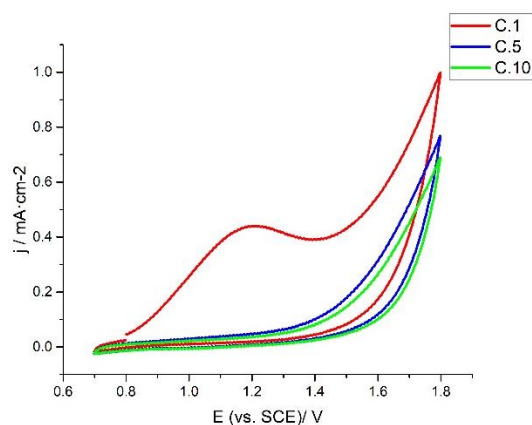
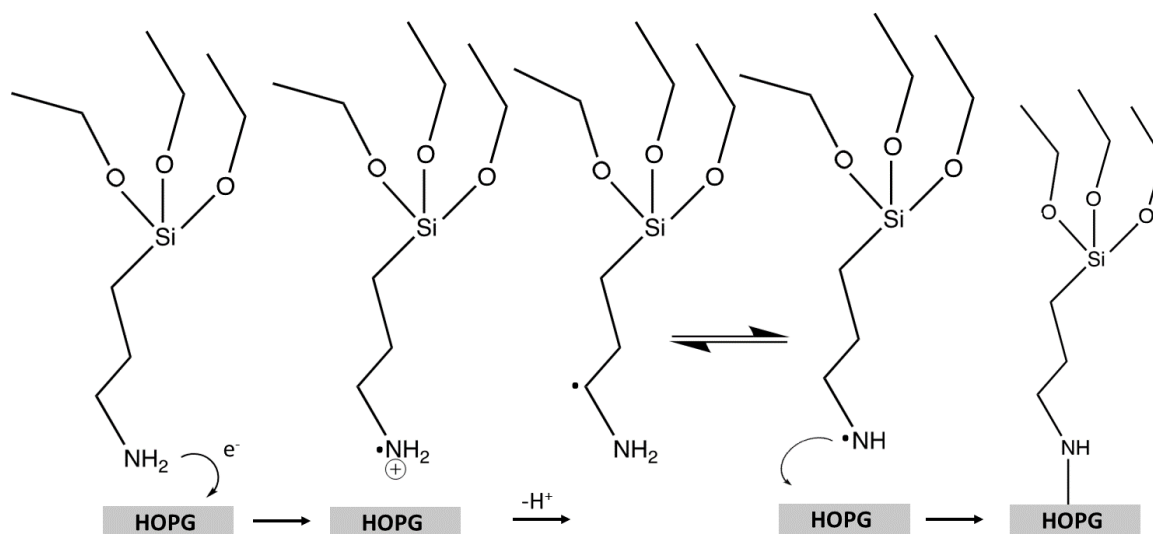


Fig 3. Cyclic voltammograms registered for the HOPG in a 1 mM APTES containing ACN solution for the amine grafting at a scan rate of 100 mV·s⁻¹. 1 (red line), 5 (blue) and 10 (green) cycles.



Scheme 3. Mechanism for the amine grafting

Characterization of the films through the silanol groups

The APTES-modified HOPG substrates were characterized by cyclic-voltammetry (CV) measurements in the presence of an electrochemical redox probe, namely ferrocyanide/ferricyanide, with the aim to obtain information about the charge-transfer properties and surface coverage after deposition of the as-prepared films. In this way, the presence of a film on the electrode surface would limit the access of the $[\text{Fe}(\text{CN})_6]^{4-}$ and $[\text{Fe}(\text{CN})_6]^{3-}$ ions to the surface. The result is shown in Fig 4, where the diffusion-controlled reversible electrochemical response exhibited by the pristine surface of the HOPG (black voltammogram) is progressively blocked by the presence of the APTES film. Thus, it is possible to observe that for increasing deposition times, the electrochemical profile becomes more irreversible (larger peak-to-peak separation and lower values of current density). The latter is attributed to the progressive formation of a more compact and denser film layer with time.

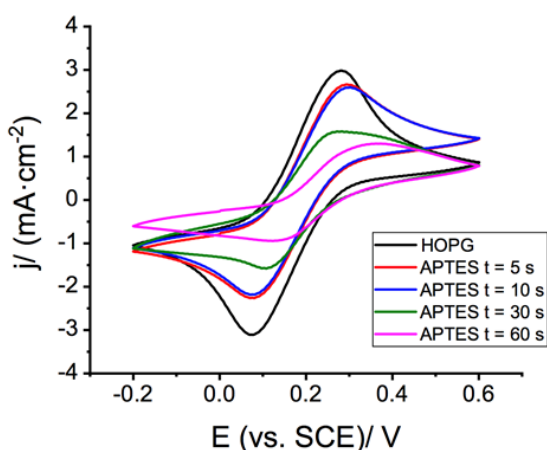


Fig 4. CV curves of the non-modified HOPG electrode (black line), after 5 s (red), 10 s (blue), 30 s (green) and 60 s (pink) deposition time of silane grafting at a scan rate of $100 \text{ mV}\cdot\text{s}^{-1}$. Recorded for $1 \text{ mM } [\text{Fe}(\text{CN})_6]^{3-/4-}$ redox couple containing 0.1 M KCl solution.

The modified electrodes were also characterized by Atomic Force Microscopy (AFM) shown in Fig 5, which allows to observe the morphology of the films, exhibiting a mostly homogeneous distribution and a reasonably good coverage of the electrode.

Since different deposition times were performed is possible to observe the growth of the layers for the

silane grafting. The results provided by AFM match the conclusions made from the cyclic-voltammetry with ferrocyanide/ferricyanide redox couple: for higher deposition times the electrode surface coverage increases. In the AFM images shown in Fig 5, it is possible to observe the formation of granular electrodeposit that gradually covers the surface of the HOPG electrode. During the initial seconds, small, rounded particles appeared both in steps and terraces, and then they start to aggregate progressively into bigger islands interconnected by granular ramified branches, which are very notorious after 60 s of deposition time. It is interesting to notice that even for the biggest aggregates it is always possible to distinguish small particles as building blocks, whose sizes increase slightly with electrodeposition time.

AFM images show the presence of 3D-hemispherical particle-like structures (see Fig S7 in SI) on the terraces (basal plane) of the HOPG surface. Their dimensions, i.e. mean particle diameter and height, increased progressively with time as can be seen in Table 1 and Figures S3 and S4 in the SI. Once the first aggregates appear modifying the surface, they continue growing until finally collapse, increasing the surface coverage as well. These APTES-based films exhibit features which are characteristic of a 3D nucleation and growth model.

Table 1. Averaged parameters obtained from cross section profiles, particle analysis, and bearing analysis carried out on the AFM images collected for HOPG surfaces after being modified in an APTES-containing aqueous solution for different deposition times.

Sample	Diameter (nm)	Height (nm)	Surface coverage (%)
t = 5 s	39.0 ± 9.5	5.9 ± 1.9	12.2 ± 1.3
t = 10 s	48.5 ± 18.2	8.2 ± 2.4	14.4 ± 2.1
t = 30 s	122.8 ± 24.5	9.1 ± 2.7	28.3 ± 5.6
t = 60 s	221.6 ± 51.4	13.5 ± 2.9	39.7 ± 8.4

Finally, an ATR-FTIR Spectrum is shown in Fig 6, in order to prove the chemisorption of the silanol groups to the surface.

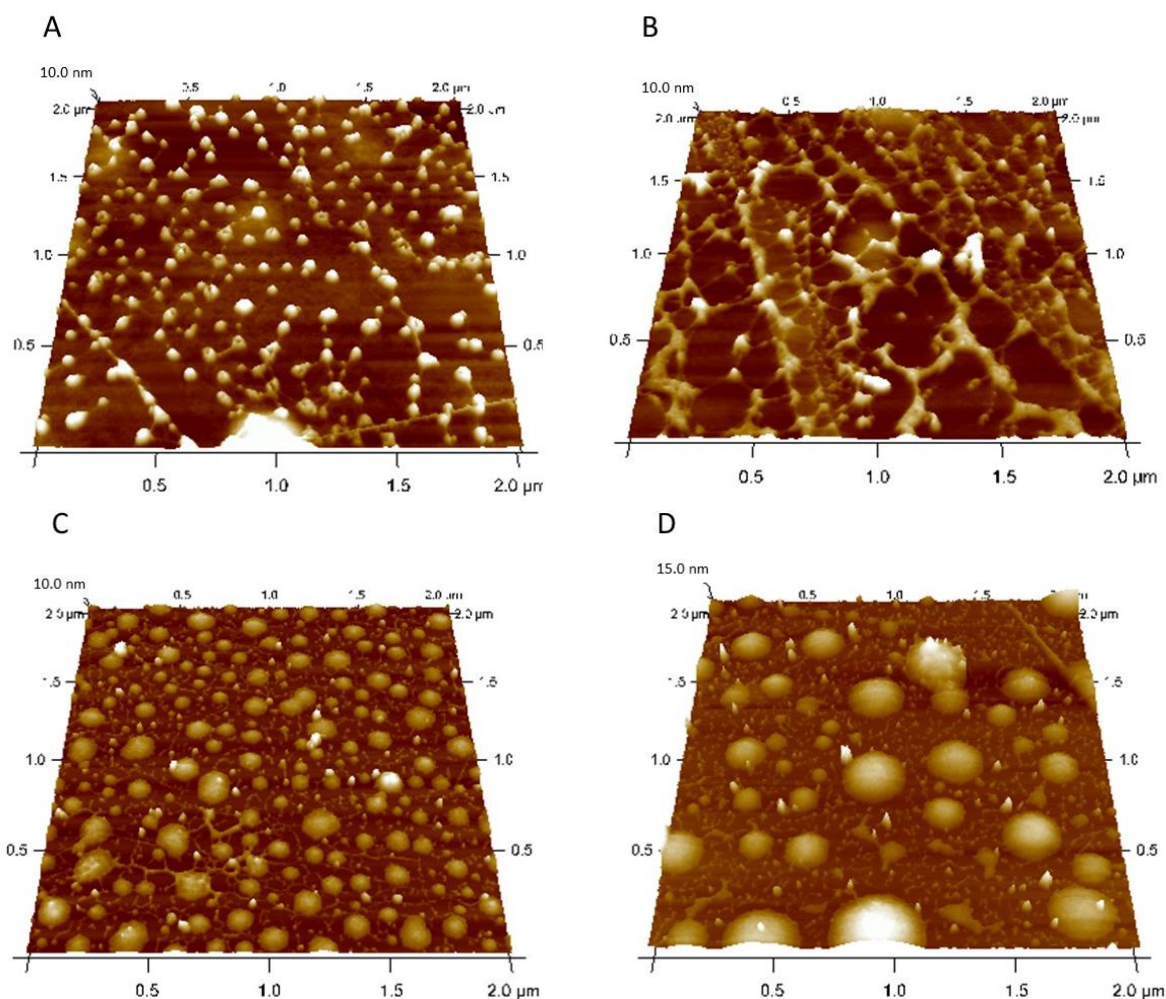


Fig 5. $2 \times 2 \mu\text{m}^2$ AFM images registered for freshly cleaved HOPG surfaces after being modified in an APTES-containing aqueous solution for different deposition times: $t = 5$ s (A), $t = 10$ s (B), $t = 30$ s (C), and $t = 60$ s (D).

The spectrum shows a broad absorption band between 1000 and 1200 cm^{-1} corresponding to the Si-O-C and Si-O-Si stretching vibrations^{45,46}, which indicate the presence of the expected siloxane network after polymerization and confirm the covalent bond between the silanol groups and the carbon atoms at the surface. The peak at 1600 cm^{-1} corresponds to the NH_2 -scissoring vibration, which confirms the presence of primary amines⁴⁷ available to allow further modifications. It is also possible to observe the corresponding carbonyl stretching band around 1720 cm^{-1} ⁴⁸. Moreover, a wide band centered at 3240 cm^{-1} is observed, that will mainly be assigned to the N-H groups⁴⁸ that appear because of the formation of the layers. The CH_2 -stretching modes appear at 2850 and 2945 cm^{-1} ⁴⁹. Finally, around 1000 cm^{-1} is possible to observe a peak corresponding to the asymmetric vibration Si-O-H⁴⁹, attributed to those Si-OH groups that do not take part of the polycondensation.

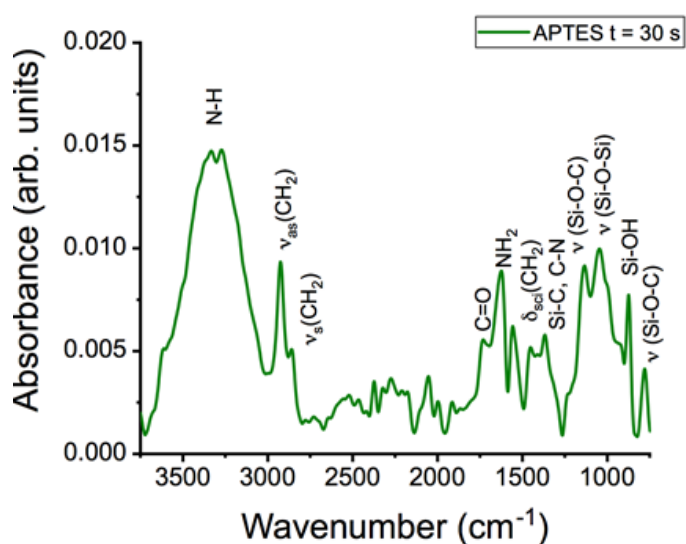


Fig 6. ATR-FTIR Spectrum obtained for the 30 s deposition time silane grafting.

Characterization of the films through the amine groups

In the case of the amine grafting, cyclic-voltammetry in the presence of the ferrocyanide/ferricyanide redox couple was performed as well, in order to characterize the growth of the layers after different cycles, showing the case for 1, 5 and 10 cycles in Fig 7. It can be shown that the coverage of the electrode surface increases with the number of cycles, showing a high coverage for the case of 10 cycles.

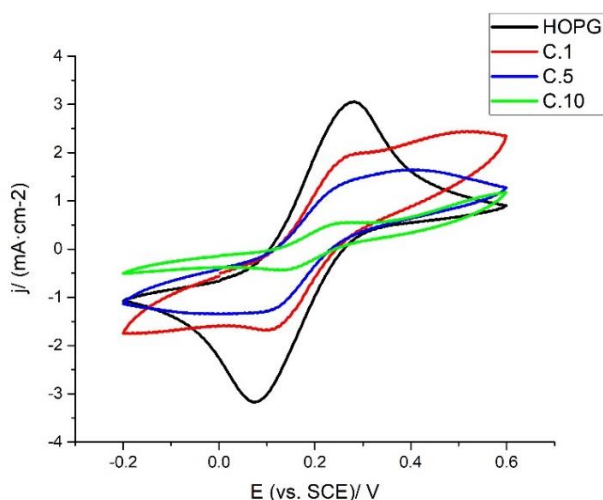


Fig 7. CV curves of the non-modified HOPG electrode (black line), after 1 (red), 5 (blue) and 10 cycles (green) of amine grafting at a scan rate of $100 \text{ mV}\cdot\text{s}^{-1}$. Recorded for $1 \text{ mM } [\text{Fe}(\text{CN})_6]^{3-/4-}$ redox couple containing 0.1 M KCl solution.

The morphology of the layers was characterized by AFM, as shown in Fig 8. In this case, the amine groups will randomly attach to the surface, forming 2D islands that will grow with the number of cycles leading to a porous compact film (see S5 and S6 in the SI). The obtained images show a layer-by-layer morphology for the growth of the film. As the number of voltametric cycles is increased, both the mean thickness of the as-formed layered APTES-based patches and the surface coverage increase noticeably, as can be seen in Table 2. Indeed, when a certain coating degree is achieved for 5 cycles, the film gets wider more rapidly. The latter is in very good agreement with the thermodynamically favored attack of radical species on molecule-modified regions in comparison to the naked HOPG substrate⁴⁴.

In this case, the morphology of the films is different than for the silane electrografting (see S7 and S8 in the SI). It

is not possible to observe here (Fig 8) the big islands that could be observed in the previous case (Fig 5D). This can be explained as follows: in the silane grafting the formation of the first nuclei would take place at the steps or defects of the terraces where the -OH functionalities are present, however, for the amine grafting, the amine radicals generated at the solid-liquid interface would randomly attach to the surface.

Finally, Raman spectra performed in order to prove the chemisorption of the amine groups to the HOPG surface are shown in Fig 9. In these spectra the G band is observed at 1580 cm^{-1} , which is attributed to the presence of hybridized C sp^2 in non-defective HOPG terraces. Interestingly, the appearance of a small hump at 1336 cm^{-1} , i.e. the D band, is originated from a hybridized vibrational mode, C sp^3 , that indicates the occurrence of defects in the original graphitic lattice structure⁵⁰. The latter confirms that the grafting process has occurred via formation of a C-N bond. The intensity ratio between the D and G bands (I_D/I_G) is considered as an indicator of the size of the graphitic domains in sp^2 carbonaceous materials⁵¹. As expected, the D/G ratio becomes more intense with the number of cycles, see Table 2. The value observed for 10 cycles would account for a certain amount of covalently attached amines to the HOPG terraces.

Table 2. Averaged parameters obtained from cross section profiles and bearing analysis carried out on the AFM images collected for HOPG surfaces after being modified in an APTES-containing ACN solution for different cycles. The ratio of the intensities of the D and G vibration bands collected from Raman spectra are presented as well.

Sample	Thickness (nm)	RMS (Sq) (nm)	Surface coverage (%)	I_D/I_G ratio
1 cycle	0.4 ± 0.1	0.4 ± 0.1	17.5 ± 2.3	-
5 cycles	0.7 ± 0.2	0.9 ± 0.2	65.2 ± 5.9	0.016
10 cycles	3.8 ± 0.4	1.7 ± 0.4	86.9 ± 9.5	0.024

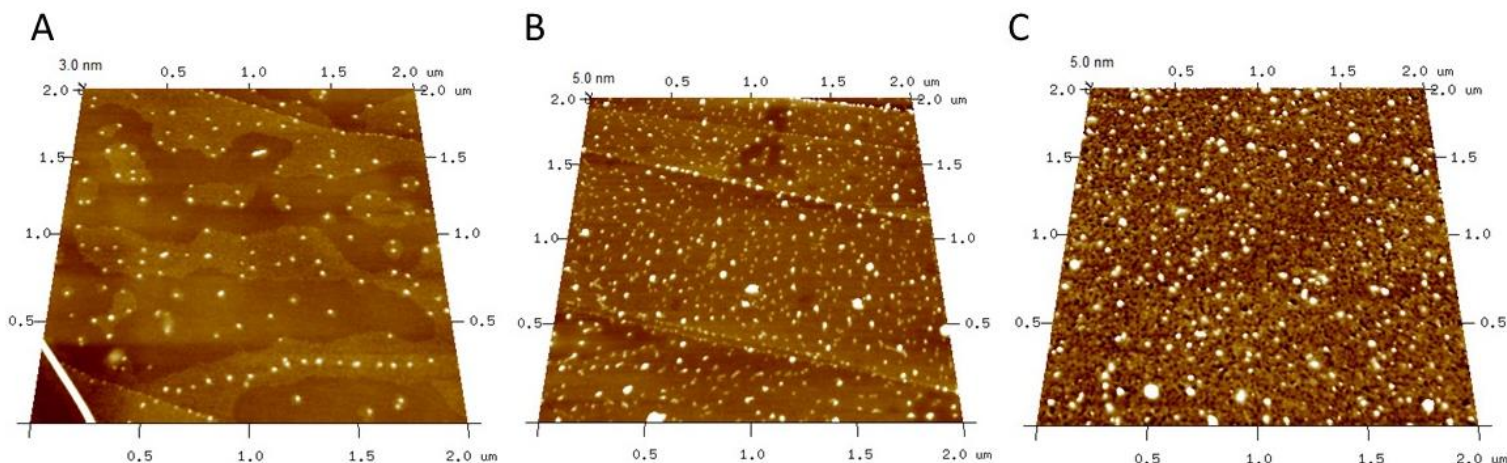


Fig 8. $2 \times 2 \mu\text{m}^2$ AFM images registered for freshly cleaved HOPG surfaces after being modified in an APTES-containing ACN solution for growing cycles: 1 (A), 5 (B), and 10 (C).

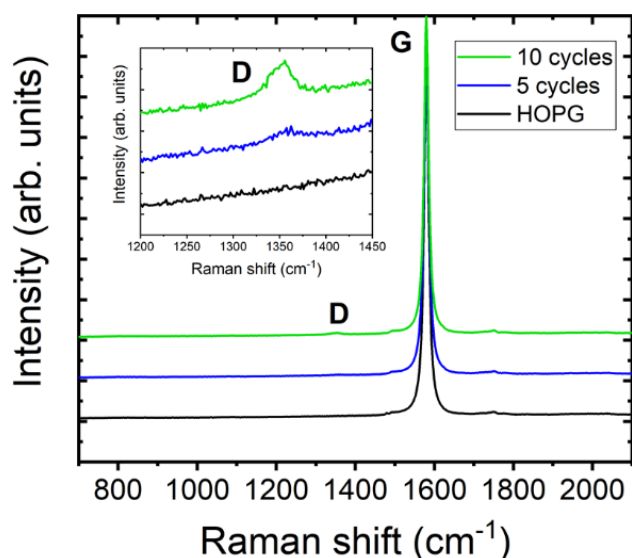


Fig 9. Raman Spectra for the non-modified HOPG electrode (black line), after 5 (blue) and 10 cycles (green) of amine grafting. Inset: Magnified view of the spectra in the range of 1200 to 1450 cm^{-1} .

Outlooks

In order to provide a more complete description of the as-prepared thin films, it would be interesting to study their mechanical and electrical (conductance and surface potential) properties and to perform contact-angle (CA) and x-ray photoelectron spectroscopy (XPS) characterization. Besides, applications to improve interfacial adhesion could be considered for both methods.

On the other hand, it could be possible to optimize the experimental conditions for the anodic (amine)

electrografting in an aqueous-based electrolyte. The latter would be related to the preparation of bifunctional of patterned APTES-based thin films with different functionalities by bipolar electrochemistry.

Conclusions

The inert surface chemistry of the basal plane of HOPG has been successfully modified by depositing APTES based ultrathin films. Given the bifunctional nature of the APTES molecule, two electrografting methodologies involving either silanol or amine groups were performed for the deposition of APTES layer. Two different morphologies were obtained according to AFM measurements: 3D-hemispherical particle-like structures interconnected by granular ramified branches (silane grafting) and a porous, layered compact film (amine grafting). They both exhibited a homogeneous size and height value distributions and a reasonably good coverage of the electrode (time- or cycle number-dependent), as has been corroborated by cyclic voltammetry in the presence of $[\text{Fe}(\text{CN})_6]^{4-}/[\text{Fe}(\text{CN})_6]^{3-}$ redox probe. The formation of Si-O-C and C-N bonds was confirmed in both cases by ATR-FTIR and Raman Spectroscopy, respectively. These modified electrodes may serve as platform for the further anchoring of bio- and macromolecules of interest in order to prepare biocompatible coatings and/or improve interfacial adhesion properties.

Acknowledgements

The author acknowledges the Spanish Ministry of Science and Innovation for the funding (ref. EQC2019-D05647-P). The author equally thanks Dr. Guillén-Villafuerte from the Research Support General Service of the ULL (SEGA) and Dr. Ródenas from the Physics Department of the ULL for carrying out the ATR-FTIR and Raman spectroscopy measurements, respectively.

References

- [1] A. Feinle, S. Flaig, M. Puchberger, U. Schubertb and N. Hüsing. *Chem. Commun*, 2015,51, 2339-2341.
- [2] P. Walker, *Journal of Adhesion Science and Technology*, 1991,5,279-305.
- [3] Abel ML. (2018) Organosilanes: Adhesion Promoters and Primers. In: da Silva L., Öchsner A., Adams R. (eds) *Handbook of Adhesion Technology*. Springer, Cham.
- [4] Zisman, W. A. *Ind. Eng. Chem. Prod. Res. DeV*, 1969, 8, 98.
- [5] Emily Asenath Smith and Wei Chen. *Langmuir* 2008, 24, 21, 12405–12409.
- [6] Franc Švegl, Jerneja Šput-Strupi, Luka Škrlep, Kurt Kalcher. *Cement and Concrete Research*, 2008, 38, 945-954.
- [7] Kanan, S. M.; Tze, W. T. Y.; Tripp, C. P. *Langmuir* 2002, 18, 6623.
- [8] Kamisetty, N. K.; Pack, S. P.; Nonogawa, M.; Devarayapalli, K. C. Kodaki, T.; Makino, K. *Anal. Bioanal. Chem.* 2006, 386, 1649–1655.
- [9] Wang, B.; Huang, Y.; Liu, L. J. *Mater. Sci.* 2006, 41, 1243–1246
- [10] Shang, Y.; Zhao, W.; Xu, E.; Tong, C.; Wu, J. *Biosens. Bioelectron.* 2010, 25,1056–1063.
- [11] Enders, D.; Nagao, T.; Pucci, A.; Nakayama, T. *Surf. Sci.* 2006, 600, L71– L75.
- [12] Balasundaram, G.; Sato, M.; Webster, T. *Biomaterials* 2006, 27, 2798–2805.
- [13] Engelhardt, H.; Orth, P. J. *Liq. Chromatogr.* 1987, 10, 1999.
- [14] Caravajal, G. S.; Leyden, D. E.; Quinting, G. R.; Maciel, G. E. *Anal. Chem.* 1988, 60, 1776.
- [15] R. G. Acres, A. V. Ellis, J. Alvino, C. E. Lenahan, D.A. Khodakov, G. F. Metha, G. G. Andersson, *The Journal of Physical Chemistry*, 2012, 116 ,10, 6289-6297
- [16] Ruiz-Cañas, M.C.; Corredor, L.M.; Quintero, H.I.; Manrique, E.; Romero Bohórquez, A.R. *Molecules* 2020, 25, 2868.
- [17] Mozetič, M. (2019). *Surface Modification to Improve Properties of Materials*. Materials, 12.
- [18] Hyacinthe Randriamahazaka, Jalal Ghilane, *Nanocarbon Electrochemistry and Electroanalysis*, 2016, 28, 13-26
- [19] D. Bélanger, J. Pinson, *Chem. Soc. Rev.*, 2011, 40, 3995-4048
- [20] S. Uchiyama, H. Watanabe, H. Yamazaki, A. Kanazawa, H. Hamana and Y. Okabe, *J. Electrochem. Soc.*, 2007, 154, F31.
- [21] G. Herlem, C. Goux, B. Fahys, A.-M. Gonc, alves, C. Mathieu, E. Sutter and J.-F. Penneau, *J. Electroanal. Chem.*, 1997, 435,259.
- [22] S. Maldonado, T. J. Smith, R. D. Williams, S. Morin, E. Barton and K. J. Stevenson, *Langmuir*, 2006, 22, 2884.
- [23] Randall S. Deinhammer, Mankit Ho, James W. Andereg, and Marc D. Porter, *Langmuir*, 1994, 10, 4, 1306–1313.
- [24] P. A. Brooksby, A. J. Downard and S. S. C. Yu, *Langmuir*, 2005, 21, 11304.
- [25] S. Fellah, R. Boukherroub , F. Ozanam and J.-N. Chazalviel , *Langmuir*, 2004, 20 , 6359.
- [26] A. Scott, D. B. Janes, C. Risko and M. A. Ratner , *Appl. Phys.Lett.*, 2007, 91 , 033508
- [27] L. Fan, J. Chen, S. Zhu, M. Wang, and G. Xu, *Electrochem. Commun.*, 2009, 11, 1823.
- [28] B. S. Flavel, D. J. Garrett, J. Lehr, J. G. Shapter and A. J. Downard, *Electrochim. Acta*, 2010, 55, 3995.
- [29] Ahmed A. Mohamed, Zakaria Salmi, Si Amar Dahoumane, Ahmed Mekki, Benjamin Carbonnier, Mohamed M. Chehimi, *Advances in Colloid and Interface Science*,225,2015,16-36.
- [30] M. A. Alonso-Lomillo, O. Rudiger, A. Maroto-Valiente, M. Velez, I. Rodríguez-Ramos, F. Javier Muñoz, V. M. Fernández and A. L. DeLacey, *Nano Lett.*, 2007, 7, 1603.
- [31] M. Kullapere, J. Kozlova, L. Matisen, V. Sammelselg, H. A. Menezes, G. Maia, D. J. Schiffrin and K. Tammeveski, *J. Electroanal. Chem.*, 2010, 641, 90.
- [32] Jiang DE, Sumpter BG, Dai S, *J. Phys. Chem. B* 2006, 110, 47, 23628–23632.
- [33] Allongue, P.; Delamar, M.; Desbat, B.; Fagebaume, O.; Hitmi, R.; Pinson, J.; Savéant, J.-M. *J. Am Chem. Soc.* 1997, 119, 201–207.
- [34] M. D'Amours, D. Bélanger, *J. Phys. Chem*, 2003, 107, 20, 4811–4817.

- [35] Barrière, F., Downard, A.J., *J Solid State Electrochem*, 2008, 12, 1231–1244.
- [36] H. Randriamahazaka and J. Ghilane, *Electroanalysis*, 2016, 28, 13-26.
- [37] A. Walcarius, E. Sibottier, *Electroanalysis*. 2005, 17, 1716-1726.
- [38] T. Nasir, L. Zhang, N. Vilà, G. Herzog, A. Walcarius, *Langmuir*. 2016, 32, 4323-4332.
- [39] N. Parhizkar, B. Ramezanzadeh, T. Shahrabi, *Applied Surface Science*, 2018, 439, 45-59.
- [40] J. Huser, S. Bistac, M. Brogly, C. Delaite, T. Lasuye, B. Stasik, *Appl. Spectrosc.* 2013, 67, 1308-1314
- [41] Behzad Rezaei, Neda Irannejad, *Electrochemical Biosensors*, Elsevier, 2019, 11-43.
- [42] Barbier B, Pinson J, Desarmot G, Sanchez M, *J Electrochem Soc*, 1990, 137:1757.
- [43] Adenier A, Chehimi MM, Gallardo I, Pinson J, Vila, *Langmuir*, 2004 20:8243.
- [44] Downard, A. J. *Electroanalysis* 2000, 12, 1085-1096.
- [45] K. Lachmann, A. Dohse, M. Thomas, S. Pohl, W. Meyring, K. E. J. Dittmar, W. Lindenmeier, C. P. Klages, *EPJ Appl. Phys.* 2011, 55, 1.
- [46] J. Borris, M. Thomas, C. P. Klages, F. Faupel, V. Zaporozhchenko, *Plasma Process. Polym.* 2007, 4, 1.
- [47] F. Truica-Marasescu, P. L. Girard-Lauriault, A. Lippitz, W. E. S. Unger, M. R. Wertheimer, *Thin Solid Films* 2008, 516, 21.
- [48] Lecoq, E.; Duday, D.; Bulou, S.; Frache, G.; Hilt, F.; Maurau, R.; Choquet, *Plasma Processes Polym.* 2013, 10, 250– 261.
- [49] Daniel A. Buttry, Jimmy C.M. Peng, Jean-Baptise Donnet, Serge Rebouillat, *Carbon*, 37, 1999, 1929-1940.
- [50] S. Niyogi, E. Bekyarova, M. E. Itkis, H. Zhang, K. Shepperd, J. Hicks, M. Sprinkle, C. Berger, C. N. Lau, W. A. deHeer, E. H. Conrad, R. C. Haddon, *Nano Lett.* 2010, 10, 4061-4066.
- [51] David López-Díaz, Marta López Holgado, José L. García-Fierro, and M. Mercedes Velázquez. *J. Phys. Chem. C* 2017, 121, 37, 20489–20497.

Supporting information.

Electrografting of 3-aminopropyltriethoxysilane on HOPG.

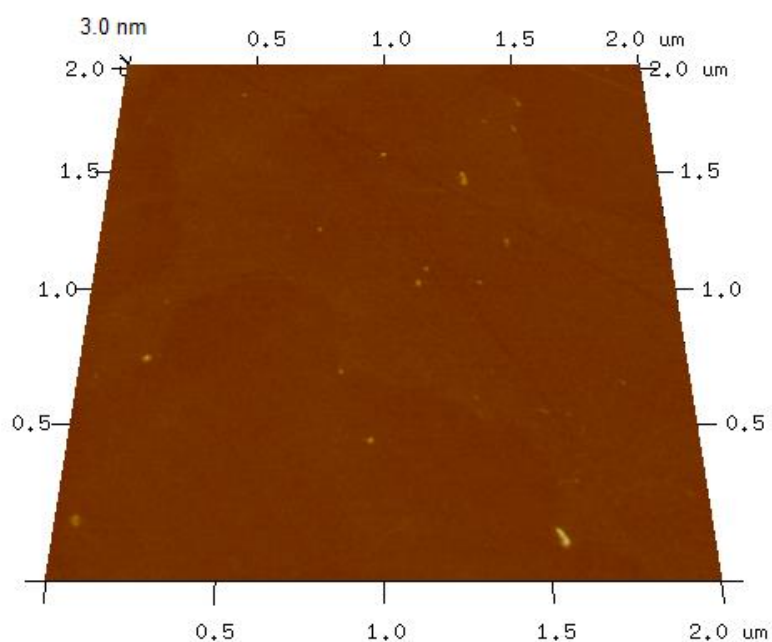


Fig S1. 2.0 x 2.0 μm² AFM image of a freshly exfoliated HOPG surface.

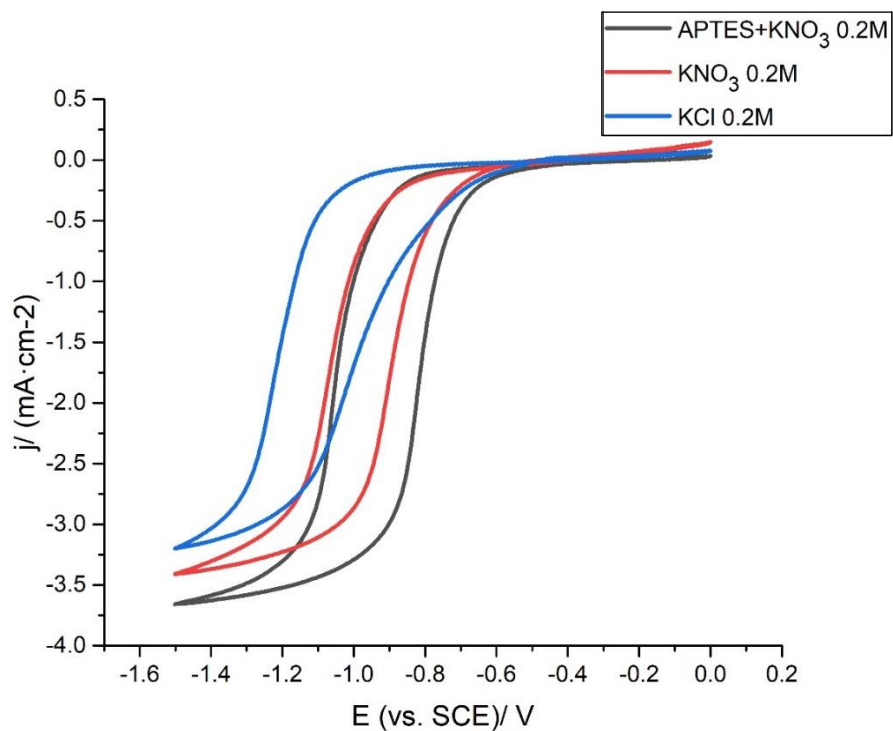


Fig S2. Cyclic voltammograms registered for the HOPG in (a) KCl 0.2 M solution (blue line), (b) KNO₃ 0.2 M (red) and (c) 1 mM APTES in KNO₃ 0.2 M (black) at a scan rate of 100 mV·s⁻¹. This figure illustrates that the reduction of the NO₃⁻ ions will have happened at -1.2 V (vs. SCE).

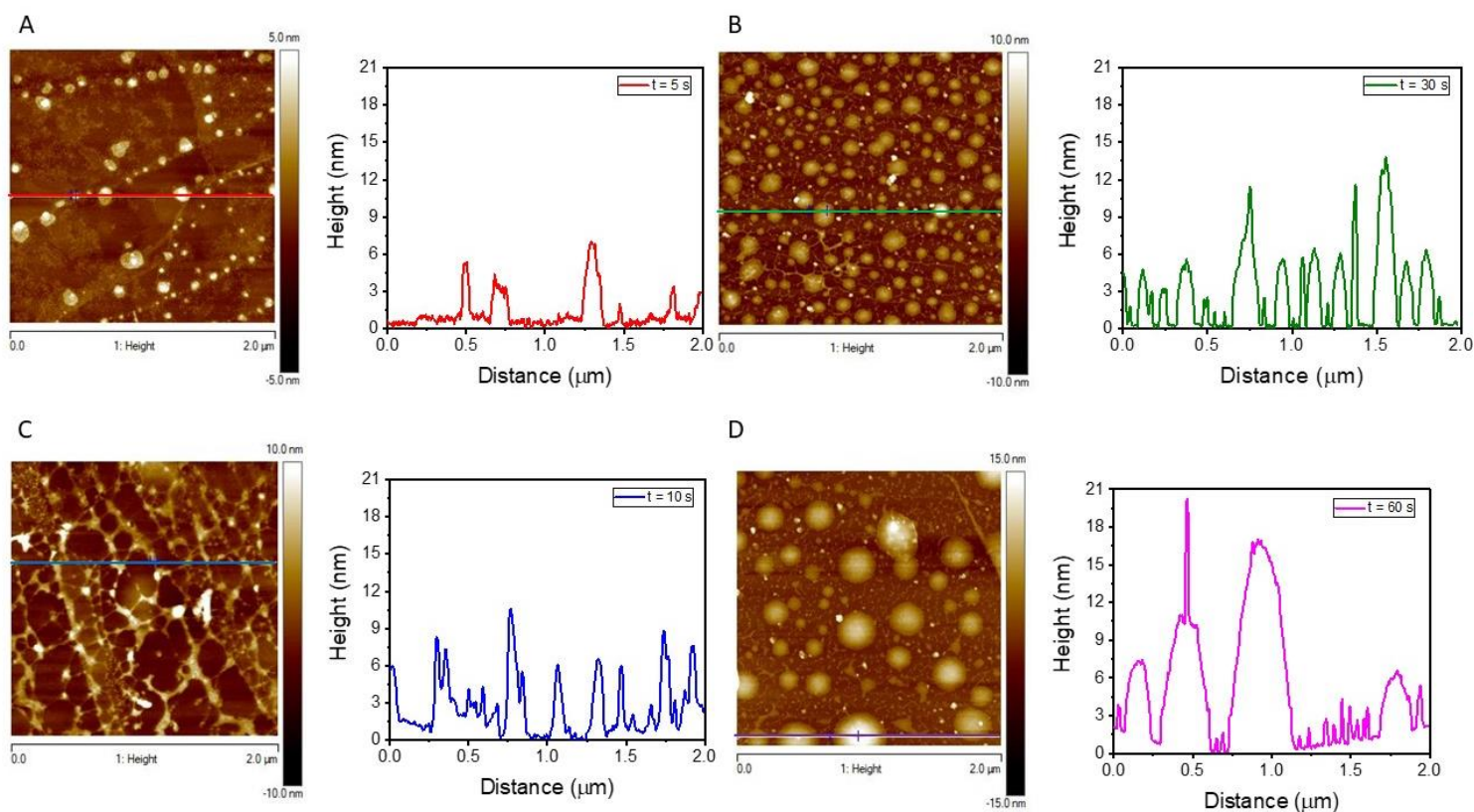


Fig S3. 2.0 x 2.0 μm^2 AFM images of the cross section registered for freshly cleaved HOPG surfaces after being modified in an APTES-containing aqueous solution for different deposition times: $t = 5$ s (A), $t = 10$ s (B), $t = 30$ s (C), and $t = 60$ s (D).

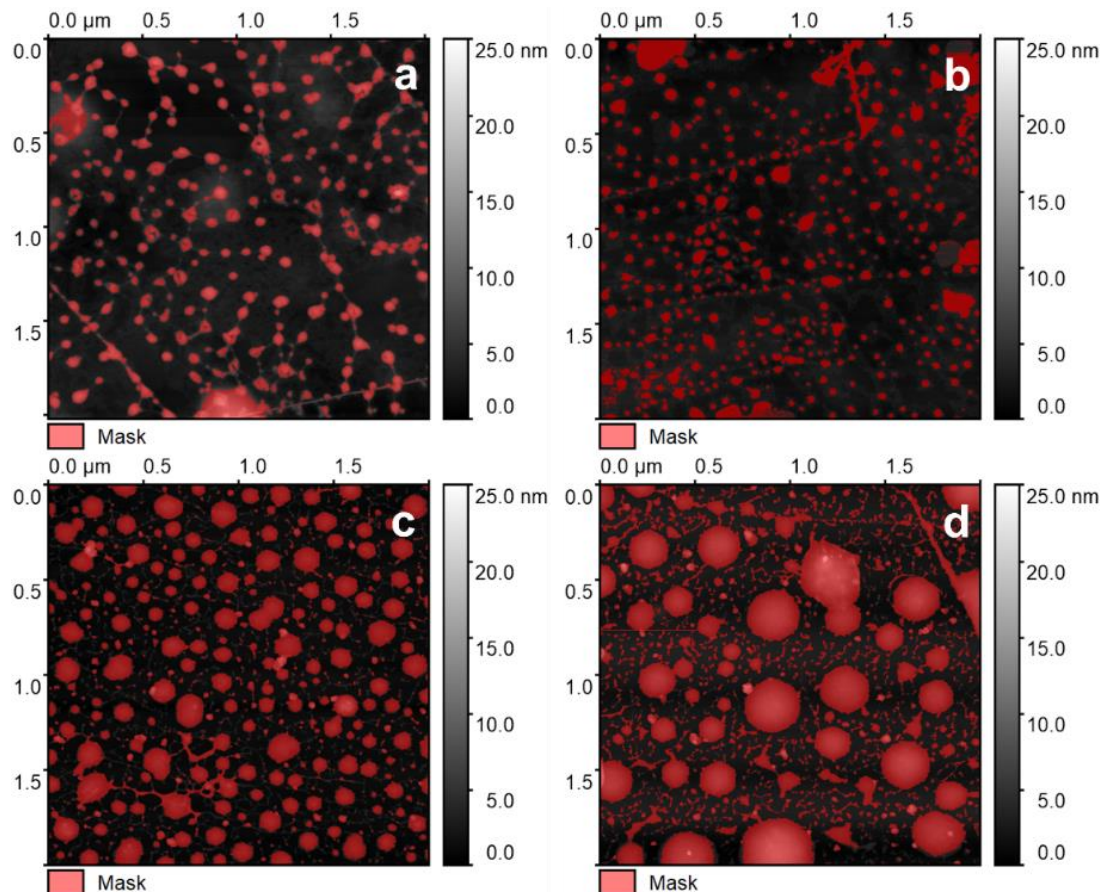


Fig S4. 2.0 x 2.0 μm^2 AFM images registered for freshly cleaved HOPG surfaces after being modified in an APTES-containing aqueous solution for different deposition times: $t = 5$ s (a), $t = 10$ s (b), $t = 30$ s (c), and $t = 60$ s (d). Red masks identify isolated APTES-based particles.

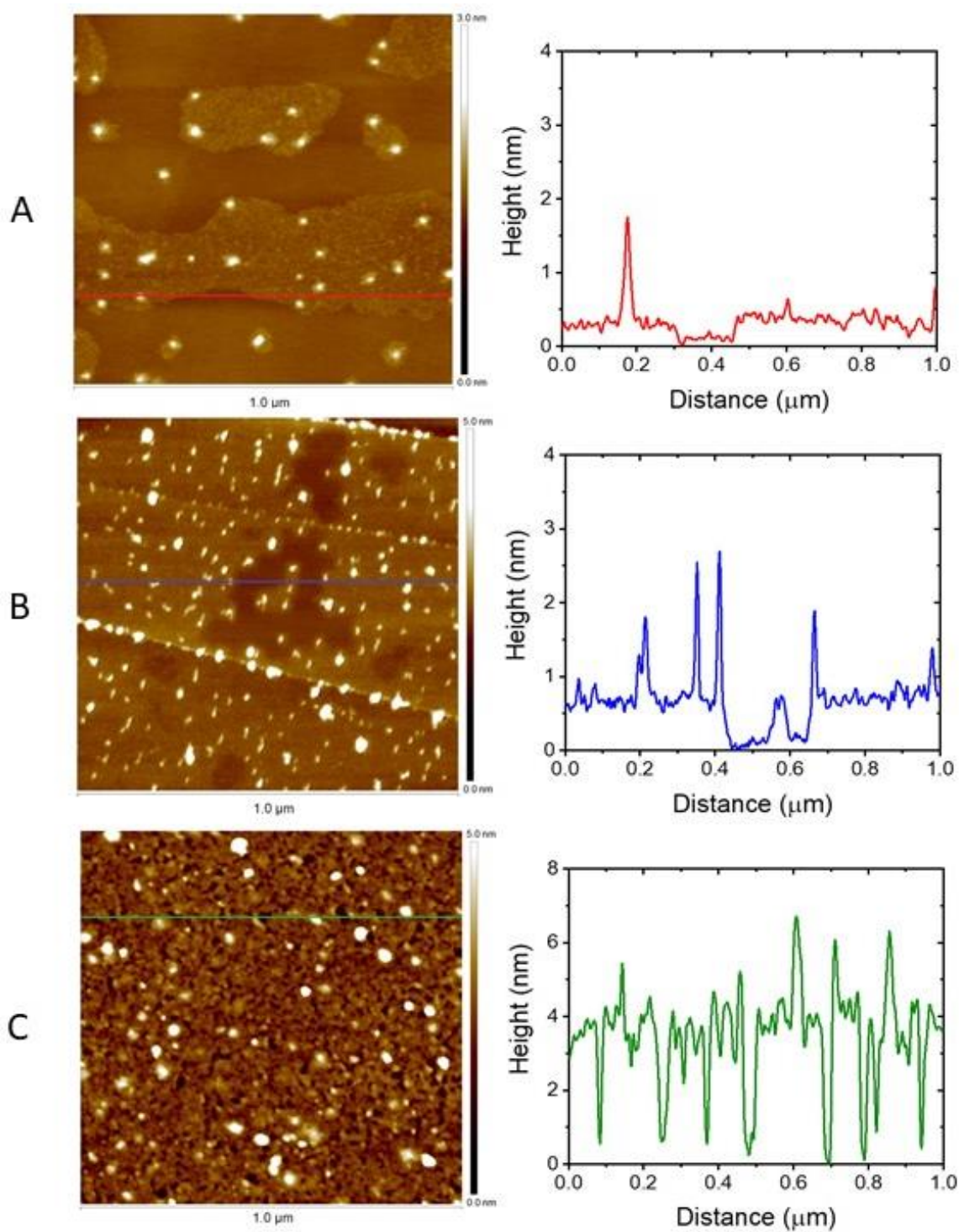


Fig S5: $2.0 \times 2.0 \mu\text{m}^2$ AFM images of the cross section registered for freshly cleaved HOPG surfaces after being modified in an APTES-containing ACN solution for growing cycles: 1 (A), 5 (B), and 10 (C).

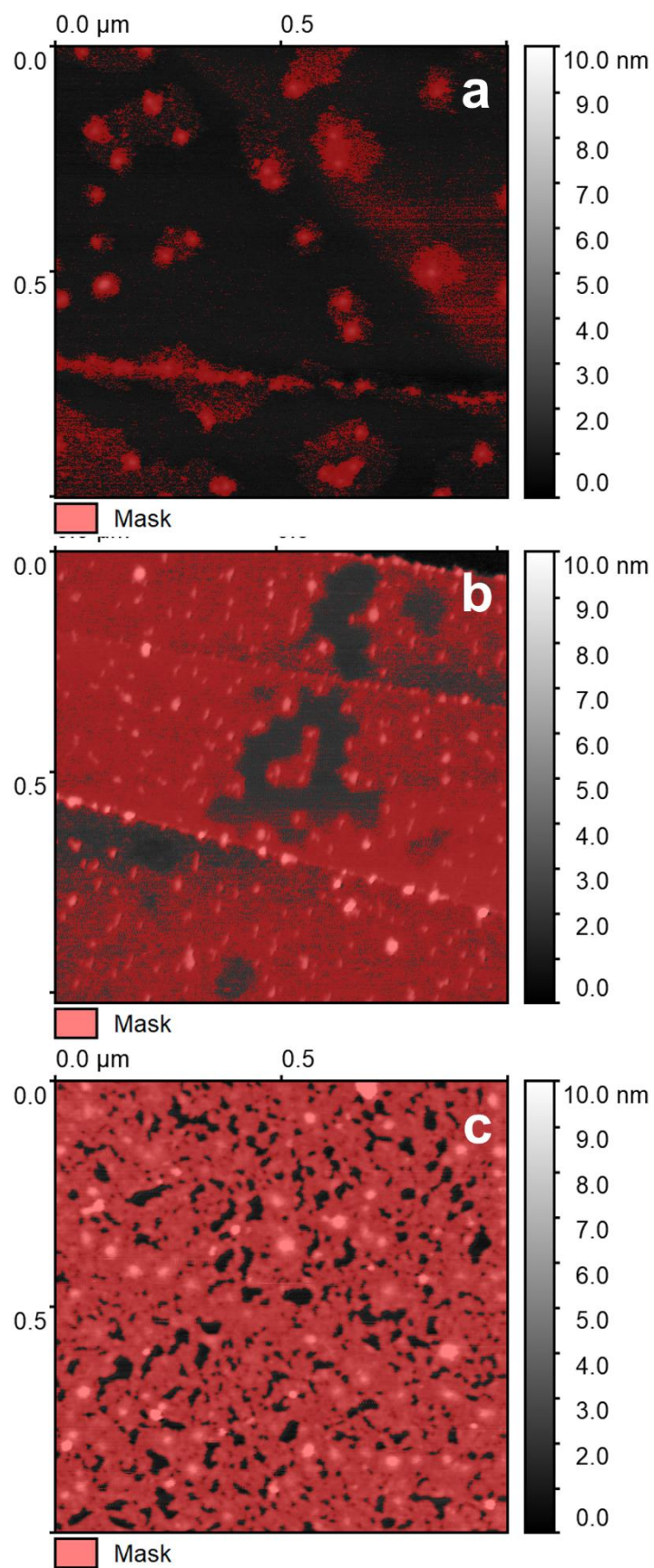


Fig S6. 1.0 x 1.0 μm² AFM images registered for freshly cleaved HOPG surfaces after being modified in an APTES-containing ACN solution for growing cycles: 1 (a), 5 (b), and 10 (c). Red masks indicate the region coated by APTES.

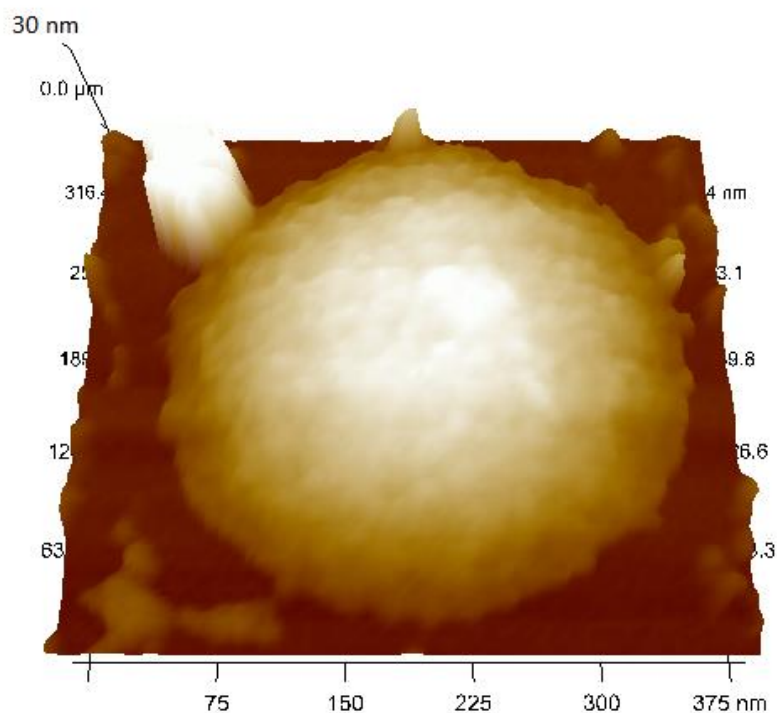


Fig S7. 375 x 320 nm² 3D AFM image registered for a freshly cleaved HOPG surface after being modified in an APTES-containing aqueous solution for t = 60 s. The zoomed image shows a 3D representation of the surface of an APTES-based hemispherical particle. The latter exhibits a corrugated morphology with pore-like features consistent with the results obtained from the electrochemical measurements.

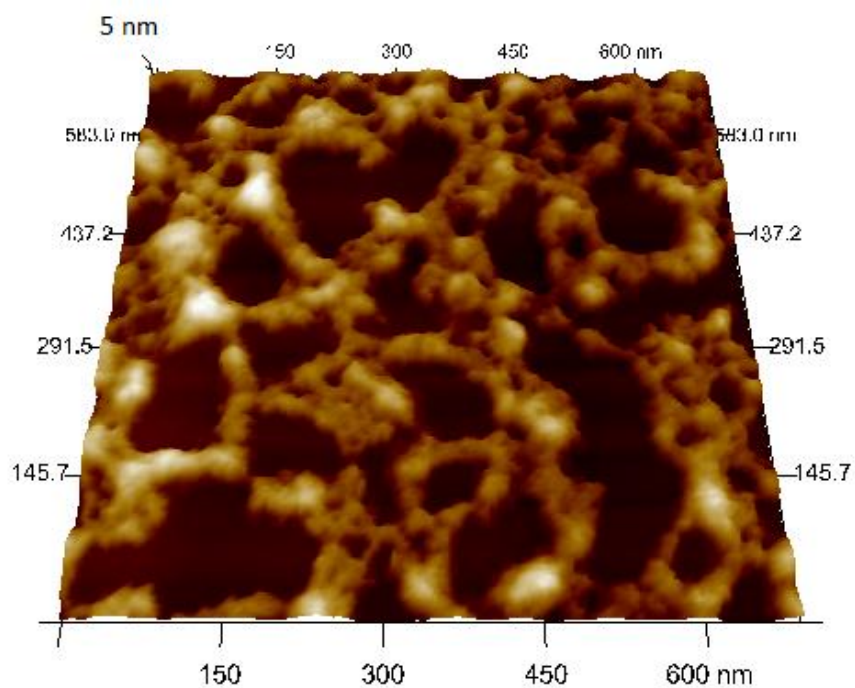


Fig S8. 600 x 600 nm² 3D AFM image registered for a freshly cleaved HOPG surface after being modified in an APTES-containing ACN solution for 10 cycles. The image shows a detail of the surface morphology.